ELSEVIER

Polymer 41 (2000) 7499–7509

polymer

Physical insight in the in-situ self-assembled films of polypyrrole

M.K. Ram[a,*], M. Adami[b], P. Faraci[b], C. Nicolini[c]

[a]*Polo Nazionale Bioelettronica, Piazza Colombo 3/5 16121 Genoa, Italy*
[b]*Polo Nazionale Bioelettronica, Via Roma 28, 57030, Marciana (LI), Italy*
[c]*Department of Science and Technology of Biophysics, Medicine and Odontostomatology (DI.S.T.BI.M.O.), University of Genoa, Via Corso Europa 30, 16132 Genoa, Italy*

Received 25 November 1998; received in revised form 24 September 1999; accepted 21 January 2000

Abstract

The ultrathin films with nanometre control over thickness and multilayered structures of polypyrrole (PPY) were manufactured by in-situ self-assembled technique. A controlled thickness of PPY was deposited on polyanion, poly(styrene sulfonate) (PSS) surfaces as a function of time; previously PSS had been deposited on various substrates (glass, mica, indium–tin-oxide coated glass plates). Later, alternate PPY and PSS films were fabricated on such substrates by the layer-by-layer technique. The films were characterized by using UV–visible, electrochemical and Quartz Crystal Microbalance techniques. The resulting morphology of the manufactured films was investigated by Atomic Force and the Scanning Tunneling Microscopies. The electrochemical surveying of self-assembled PPY films in different electrolytic media highlighted the sensor application. Typical supramolecular films of PPY/PSS were found to have conductivity values in the range of 10^{-2}–10^{-1} S/cm.

Keywords: Polypyrrole; Self-assembly; Layer-by-layer

1. Introduction

Ultrathin organic films are currently gaining interest in many areas such as integrated optics, biosensors, chemical sensors, friction reducing coating, surface orientation layers and molecular electronics [1–8]. Most of the applications require well-defined films composed of molecules with tailor-made properties in unique spatial arrangements with respect to each other and to the substrates [9–11]. Recently, a new technique of constructing multilayer assemblies by consecutively alternating adsorption of anionic and cationic polyelectrolytes was developed, where the adsorption process was independent of the substrate size and topology [12–14]. This technique was originally developed by Decher for polyelectrolytes, and later extended to doped conjugated polymers by Rubner and co-workers [15–24]. Molecular-level processing of various conjugated polymers (i.e. polypyrrole (PPY), polyaniline, poly(phenylene vinylene), poly(*o*-anisidine)) by layer-by-layer (LBL) technique has been shown in the literature [25–32].

Among conducting polymers, PPY is one of the extensively studied electronic materials, and thus has received much attention because of various technological applications [32–37]. Though PPY receives considerable interest, processing it into an ultrathin film is a challenging task because of its intractability, insolubility and infusibility in most of the common organic solvents [26–31,37]. PPY is usually synthesized by electrochemical and chemical oxidative polymerization techniques. Its physical and chemical properties are considerably dependent upon the dopants and polymerization conditions. Recent evidence shows that PPY can be self-assembled into multilayer thin films with a suitable polyanion [26–31]. In order to highlight the attractive features of self-assembly, no dedicated and sensitive equipment is needed and the adsorption can be carried out from aqueous solutions using a polyanion such as the sodium salt of poly(styrene sulfonate) (PSS) [38–41]. The anion *p*-toluene sulfonate (PTS) was used; this is poorly nucleophilic but permitted the formation of good quality PPY films.

Beginning with these considerations, the main aims of this work were to analyse the fabrication and the characterization of in-situ self-assembled films of PPY, as well as to investigate the effect of electrolytes in the electrochemical and electrical properties of the films. The PPY films were fabricated on a polyanion, PSS coated substrates (glass, mica and indium–tin-oxide coated glass plates), as a function of time. The LBL technique was also used to fabricate

* Corresponding author. Tel./fax: + 39-10-532890.
E-mail address: manoj@ibf.unige.it (M.K. Ram).

0032-3861/00/$ - see front matter
PII: S0032-3861(00)00078-1

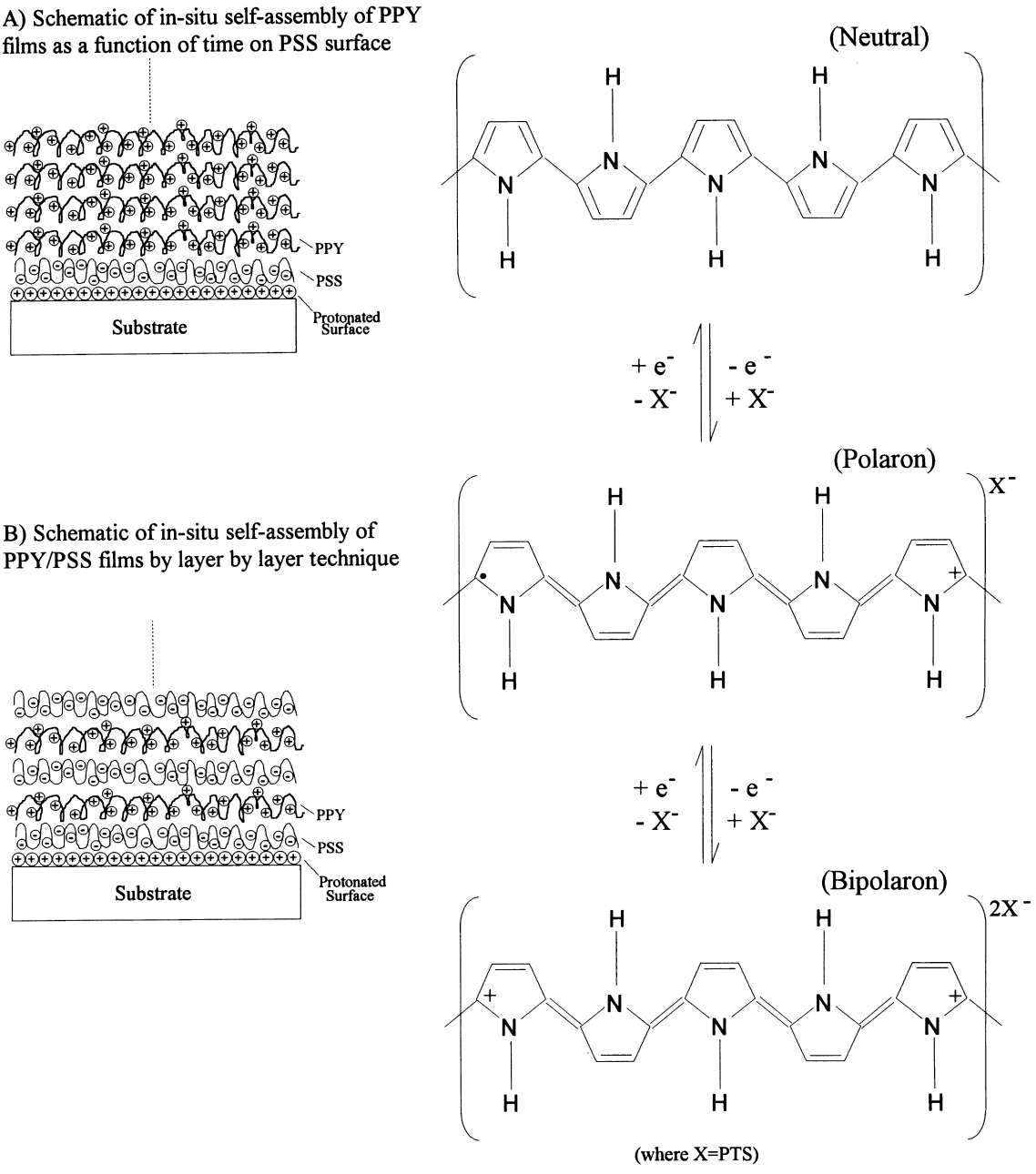

Fig. 1. (a) Schematic of in-situ self-assembled layer-by-layer films of PPY with PSS. (b) Schematic of in-situ self-assembly of PPY on PSS surface as function of time.

alternate PPY and PSS layers on such substrates. The UV–visible, electrochemical, Quartz Crystal Microbalance and electrical conductivity techniques were used to characterize the in-situ self-assembled films of PPY, and the resulting morphology was investigated by Scanning Probe Microscopies. The electrochemical investigations on such films were performed in different electrolytic media. The electrical characterizations gave evidence of the change in conductivity, which can be applicable as a sensor of protonic acid.

2. Experimental details

2.1. Preparation of the substrates

Substrates were activated following a procedure reported previously [26–31]. The reported procedure produced a surface with covalently anchored amine group (positively charged surface) [26–31]. The indium–tin-oxide (ITO) coated glass was first washed with methanol/chloroform, and later treated with aqueous ammonia for 5 min to create

the hydrophilic surface. The positively charged surface on ITO coated glass plate was created similarly to the glass treatment. Such substrates were preserved in deionized water before the deposition of in-situ self-assembled LBL films. The substrates kept in deionized water can be used for a period of 2–3 days.

2.2. In-situ self-assembly of PPY

The sodium salt of poly(styrene sulfonate) (PSS, $M_w = 70,000$) at 2 mg/ml was dissolved in water, and adjusted to pH 1 by addition of HCl. The positively charged substrate was dipped into PSS solution for 10 min to obtain a negatively charged surface. Later, the PSS coated substrate was washed in deionized water and dried by blowing on it with nitrogen gas. The PSS coated substrate was suitable to fabricate the PPY film, where simultaneous polymerization of the pyrrole monomer and oxidation of the PPY molecules occurred. The active solution for PPY contained the oxidizing agent (ferric chloride, $FeCl_3$) and *p*-toluene sulfonic acid (PTS) and was later adjusted to pH 1 by HCl followed by the addition of pyrrole monomer. The various concentrations of the dipping solutions of pyrrole monomer along with PTS and $FeCl_3$ were tested. The polymeric charge in solution was evidence of the effect of pH on the active solution. The optimum films of PPY were achieved through a solution containing 0.006 M $FeCl_3$, 0.026 M PTS and 0.02 M pyrrole, as shown in literature [26–31]. The active solution was stirred for 15 min after the addition of the pyrrole monomer and then filtered. Such filtered solutions were used for the deposition of the PPY film. A schematic drawing of the procedure is sketched in Fig. 1a. A single layer of PPY was obtained in 5 min by the in-situ polymerization. Alternating the dipping of the protonated substrate in PSS and PPY solutions produced bilayered structures. The alternate bilayers of PSS/PPY were fabricated by dipping the protonated substrates in PSS solution for 10 min, and 5 min in PPY active solution followed by washing and drying in each step of deposition. The schematic of LBL deposition of PSS and PPY films is shown in Fig. 1b.

2.3. Optical measurements

The optical properties of in-situ self-assembled films of PPY deposited onto PSS/glass plates as a function of time, and alternate bilayers PPY/PSS films were measured by UV–visible spectroscopy (Jasco spectrophotometer model 7800). Absorption optical spectra allowed determining the inclusion of dopant in the polymer as well as evaluation of the band gap of the PPY self-assembled films.

2.4. Quartz crystal microbalance (QCM) measurements

The samples were tested by using a home-built nanogravemetric apparatus in order to observe the relationship between deposition time and thickness. A different number of layers were transferred onto 10 MHz AT-cut quartz crystal microbalances containing the gold electrodes (Nuova Mistral, Italy), and the decreasing resonant frequency was analysed. The frequency variation was correlated to the mass change of self-assembled films by using the Sauerbray equation [42–44]:

$$\Delta m = K\Delta f \quad (1)$$

The constant K depends upon the physical parameters of the utilized resonator, which defines the sensitivity of the instrument. The value of K was estimated to be 0.587 ng Hz^{-1} mm^{-2}, where the frequency 'Δf' was in Hz and the mass density 'Δm' was in ng mm^{-2}.

2.5. Surface characterization

The surface morphology of the PPY films was investigated by an Atomic Force Microscope (AFM), which was a home-built instrument (Polo Nazionale Bioelettronica) working in contact mode in air at a constant contact force [26–31,42–44]. A commercial instrument (Asse-Z, Italy) performed the STM analysis of PSS/PPY films. The STM was equipped with a small scanning range piezo tube to achieve the high-resolution images of the samples.

2.6. Electrochemical measurements

The potentiostat/galvanostat (EG & G PARC, model 163 with the supplied software M270) was used to measure the electrochemical measurements. A standard three-electrodes configuration was used, where PPY films on ITO coated glass plate served as a working electrode, platinum as a counter and Ag/AgCl as a reference electrode. The cyclic voltammograms (CVs) of PSS/PPY films were measured at different concentrations of electrolytes.

2.7. Electrical measurements

The computer-controlled electrometer (Keithley model 6517) was used to characterize the electrical properties of the PPY films. Current–voltage (I–V) characteristics were obtained by a potential step of 0.05 V to the films deposited on interdigitated electrodes. The interdigitated electrodes were fabricated on a quartz plate by the photolithography technique [26–31]. Pairs of electrodes were spaced at 50 μm, a width of 50 μm and a height of 40 nm.

3. Results and discussion

3.1. Role of PSS in the formation of the film

The polyanion PSS layer on the substrate plays a crucial role in the formation and the polymerization of polycation PPY molecules. The polyelectrolytes are known to adsorb strongly to oppositely charged surfaces. There is a continuous formation of PPY because of the chemical oxidation of the monomer pyrrole in the presence of $FeCl_3$. Due to the

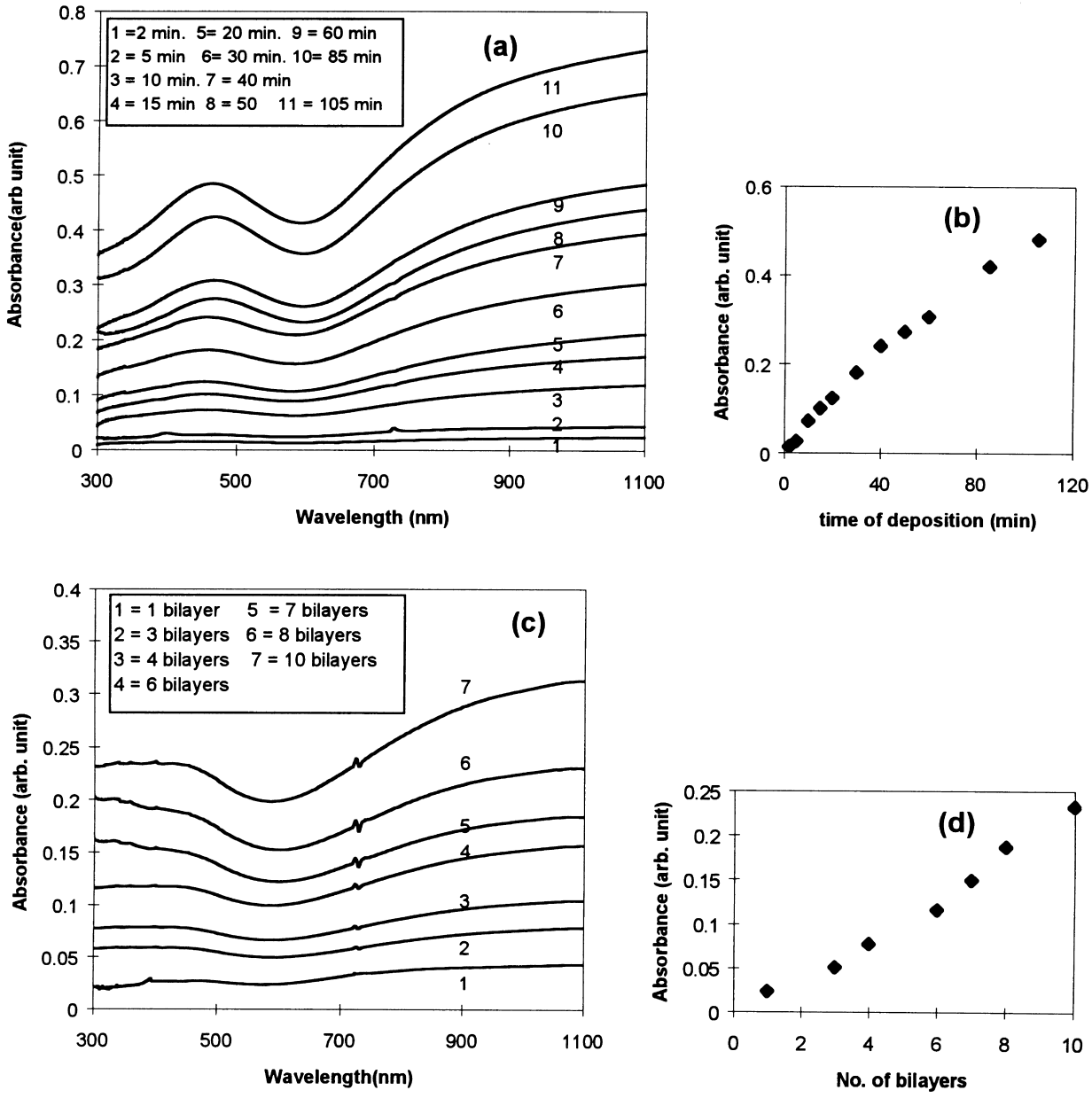

Fig. 2. (a) UV–visible absorption of in-situ self-assembled PPY films on PSS surface deposited on glass substrates as function of time. (b) UV absorption vs. self-assembled PPY films on PSS surface at 450 nm. (c) UV–visible absorption of in-situ self-assembled layer-by-layer films of PPY and PSS. (d) UV–visible absorption vs. number of PSS/PPY bilayers at 470 nm.

electrostatic interaction between Fe^{+3} and PSS polyelectrolytes, it causes a local perconcentration of both pyrrole and Fe^{+3}, and thus enhances the polymerization rate. The in-situ polymerized PPY molecules being polycation are attracted towards polyanion PSS chains via hydrophobic interaction resulting in a higher local concentration. Polymerization can also be enhanced by the low concentration of $FeCl_3$ in the active solution [45]. The higher concentration of $FeCl_3$ brings about a higher conductivity value of PPY, but the controlled polymerization is always possible at low concentration of $FeCl_3$. It was observed that the polymerization of PPY occurs poorly on the surface of the reaction vessel, and is easily washed by the flow of water. The PPY films in conducting form contains 10–35% by weight of the anions [38–41]. Dipping time and solution chemistry can therefore control the thickness of the deposited layer.

3.2. Optical characterization of PSS/PPY bilayers film

UV–visible spectroscopy was chosen to analyse the optical bands and uniformity of PPY films. Fig. 2a shows the UV–visible absorption of PPY films deposited on PSS surface as a function of time. It reflects the typical spectra of PPY at 450 nm and broad band at 940 nm indicating the

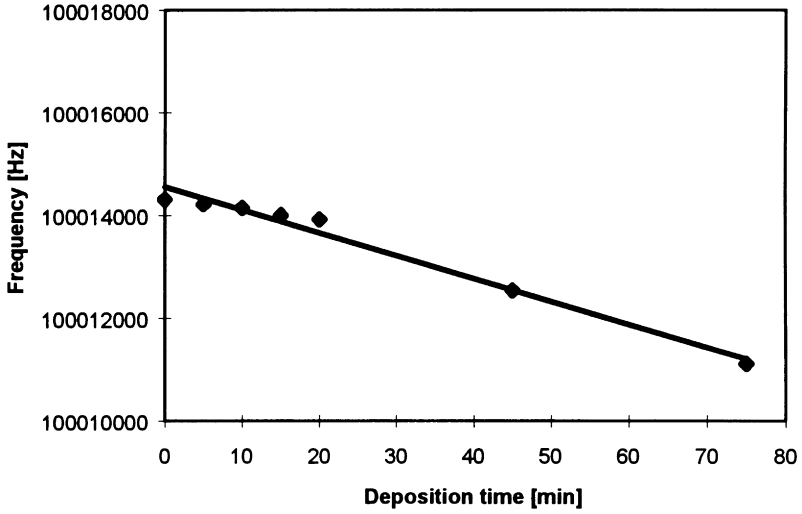

Fig. 3. Relationship between frequency variation and time deposition of PPY samples deposited onto 10 MHz quartzes.

degree of doping of PPY films. Such doping of PPY films is considered in the context of charge carriers responsible for the electronic conductivity in the doped PPY as shown in Fig. 1. The peak at 450 nm is also found in literature for the electrochemical PPY films [46–48]. The single layer deposition process described here has been used to create the films of nearly 60–200 Å. The UV–visible absorption magnitude at 450 nm as a function of deposition time is shown in Fig. 2b. The in-situ polymerization of the PPY film is a dynamic process where the thickness of the PPY films initially increases linearly to the time, and then gradually evidences to non-linear deposition after 60 min, as shown in Fig. 2b. The remaining PPY, i.e. not deposited on the surface of the substrates, precipitated gradually out of the active solution. Fig. 2c shows the UV–visible absorption as a function of PSS/PPY bilayers. Interestingly, it depicts the UV–visible absorption peak at 470 nm as shown in Fig. 2c. The change in optical absorption from 450 to 470 nm is also observed for the alternate PSS and PPY deposited LBL film. The nature of the PPY film formation in both cases is the in-situ self-assembly, but the mechanisms are different. The nature of absorption processes in the both cases could have caused different orientation of the molecular structure of PPY conducting polymer. It shows a highly reproducible thickness of PPY added for each interval of 5 min. Fig. 2d depicts a linear increase in the UV–visible absorption magnitude at 470 nm as a function of the number of bilayers for PSS/PPY films. Though the PSS film is formed by the deposition of 10 min, its overall thickness does not contribute in the absorbance of film. The UV–visible absorption study reveals nearly equal absorption magnitude in each deposition and attributes to highly reproducible type of deposition. The band gaps of PSS/PPY bilayers and PSS and PPY as a function of time on different substrates were calculated using a one-dimensional equation [46–48]. The band gap was estimated by extrapolating $(1/\alpha h\nu)^2$ vs. photon energy ($h\nu$) curve and has been estimated to be 2.65 eV for the films made as a function of time, whereas LBL deposited films with PSS show the band gap at 2.7 eV. The optical adsorption edge at 2.2 eV is also determined. PPY shows 95% amorphous and 5% crystalline structure in the doped state [46–48]. The absence of crystallinity in the doped PPY makes the band edge blunt similar to any amorphous semiconductors, and the band edges contain tails with a reasonable density of states. This could have caused the band gap to vary within a range of 3.1–2.6 eV. The band gap in the self-assembled PPY films has been found to be less than the electrochemical films and shows a band gap of nearly 3.1 eV [46–48].

Table 1
QCM parameters of layer-by-layer films of PPS/PPY films

Number of bilayers	Change in frequency (Δf), Hz	Change of mass (Δm), g
1	43	7.3×10^{-8}
2	298	5.1×10^{-7}
3	557	9.5×10^{-7}
4	757	1.3×10^{-6}

3.3. QCM studies

This technique allows characterization of the uniformity of the film by measuring the frequency change (that can be computed to mass change) in each successive deposited layer on the quartz crystal. The in-situ self-assembled films of PPY were measured in ex-situ measurement procedure. Initially, the PSS film was deposited on quartz crystal, and the QCM study was performed. Later, such substrate was dipped for the 5 min in PPY solution, rinsed, dried and measurements were performed. The similar procedure was repeated for the number of PSS/PPY bilayers. Fig. 3 shows a linear dependence of the frequency shifts vs. the deposition time of PPY films on PSS coated quartz plates. It thus

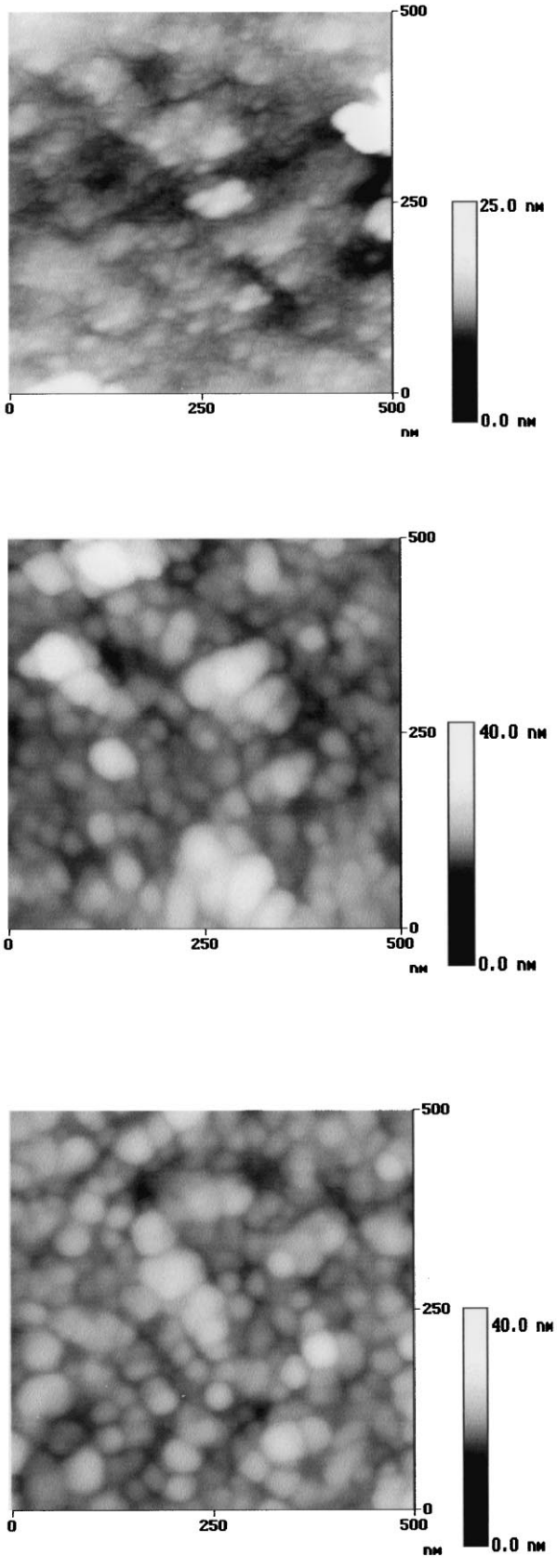

Fig. 4. AFM image of the in-situ self-assembled films of PPY deposited as function of time: (1) 2 min; (2) 10 min; (3) 40 min. The size of the each image is 500 nm × 500 nm.

reveals a linearity in the deposition of PPY films as a function of time. Table 1 shows a similar result in the case of alternating deposition of PSS/PPY layers. The corresponding mass variation was calculated as shown in Table 1.

3.4. Surface characterization of PPY films

The uniformity in the deposition process and surface morphology of the deposited films are observed by AFM studies. Each picture is representative of various samples, since similar images were found in four different regions of the samples. Fig. 4 shows the surface morphology of in-situ self-assembled films of PPY fabricated on a PSS surface on glass plates as a function of time, i.e. (1) 2 min, (2) 10 min and (3) 40 min, respectively. The size of each of the image is 500 nm × 500 nm. The AFM images reveal a surface topography of typical granular patterns and the size of spheres are ranging from 6.0 to 42.1 nm depending upon deposition time of the films. The PPY films adsorbed for 2 min shown in Fig. 4 have imperfections in packing, whereas the linearity of multilayer growth indicates that the thin system is self-healing with respect to addition of subsequent layers. It is possible to see fine granular sizes in self-assembled films of PPY films, and such dimension of the grains was never been observed in the electrochemical films [49–51]. Although it has been impossible to know the real organization of the polymer at the PSS/substrate or in the PPY/PSS structures, AFM studies speculate about the uniformity and equal grains distributions in each successive deposition. Table 2 shows the AFM parameters of such deposited PPY films. The films of PPY started forming as soon as the PSS coated substrate was introduced into the active solution, whereas the complete covered films with fine grains appeared after 5 min. The STM analysis evidenced circular shaped, with average diameter of 22 nm, grains for 20-min self-assembled films on graphite surface in Fig. 5. It has a size of 0.5 × 0.5 μm. It can be highlighted that surface measurements show a topography of typical spherical or granular patterns ranging from 6.0 to 42 nm depending on the film thickness and length of deposition time. Such surface morphology could be due to the orientated PPY molecules on the substrate [49–51]. The AFM image of PSS/PPY bilayers shows films with a similar structure as well (figure not shown). The thickness of the films is also estimated via AFM imaging of the samples.

3.5. Electrochemical surveying

The electrochemical investigation of in-situ self-assembled films of PPY was carried out by deposition on PSS/ITO coated glass plates. The cyclic voltammograms (CVs) of PPY films deposited on a PSS/ITO glass plate for 45 min are shown in Fig. 6. PPY/PSS/ITO acted as working electrode, platinum as counter electrode and Ag/AgCl as reference electrode in a solution containing 0.1 M KCl at a scan rate of 5, 10, 20, 25, 50, 100 mV/s as shown in Fig. 6. The potential was scanned between −0.8 and 0.8 V

Table 2
AFM parameters of PSS/PPY films deposited as a function of time

Deposition as a function of time #	RMS (nm) roughness	DZ (nm)	Size cluster circular (ϕ) nm	RMS/DZ (%)
3	1.2	6.0	54 ± 26	20
10	1.2	42.1	32 ± 11	9
25	2.1	29.8	29 ± 20	9
40	2.1	33.1	29 ± 17	10
60	2.3	11.8	36 ± 12	10

vs. Ag/AgCl. The obtained redox peaks at potentials of −261.8 and −355.5 mV are the characteristic peaks of a PPY film. The peak at −355.5 mV is related to the movement of Cl^- ions, and has been assigned to the uptake of proton transfer. The potential of redox peaks is related to the doping and dedoping of Cl^-. The redox potential peaks do not shift with the scan rate [52–55]. The shape of the reduction peak is different from that of the electrochemical by synthesized PPY films. In a surface confined species, the redox peak potential current (I_p) is proportional to square root of scan rates (V) [53]. The I_p vs. $V^{1/2}$ shows a linear relationship between redox peak current and $V^{1/2}$, and reveals a diffusion-controlled oxidation of PPY films (figure not shown). The diffusion coefficients in the redox system have been calculated as 1.13 and 3.13 cm^2/s, respectively.

The counter ions and potential scanning range influence strongly the electrochemical properties of the PPY films. With this consideration, PPY film was scanned from −0.8 to 1.5 V (in some cases) in different electrolytic media. Interestingly, the potential of the redox peaks and the shape of CV are observed differently in each electrolytic medium. The shape dependent CV in different electrolytic media can also be seen in the literature for electrochemically grown PPY films [53]. Fig. 7 shows the CV of self-assembled PPY films on PSS/ITO coated glass plates for 30 min. The cyclic voltammograms evidence different values of redox potentials in each studied electrolyte as shown in Table 3. The peaks of redox potentials are also different than the electrochemically grown PPY films [26–31]. The redox potentials ≥1.0 V can be due to the over oxidation of the PPY films. It is apparent from Table 3 that the redox reactivity of PPY strongly depends on the dopant as well as the electrolyte during cyclic voltammetry (CV). The CV studies reveal peaks at more than one redox peak potential over such a wide range of potential value [53], and demonstrate that the redox activities of the films mostly depend on the dopant ions. The films show degradation and low current in the CV for potentials exceeding more than 1.2 V vs. Ag/AgCl.

3.6. Electrical conductivity on PPY samples

Electrical measurements on PPY films deposited on various types of substrates were performed. Initially, the

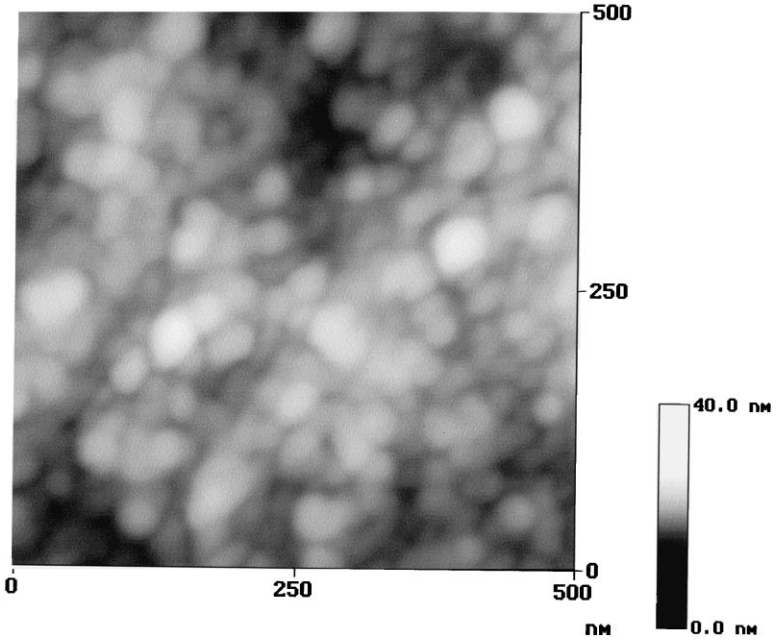

Fig. 5. STM pictures for the in-situ self-assembled films deposited for 20 min. The image size is 0.5 × 0.5 μm.

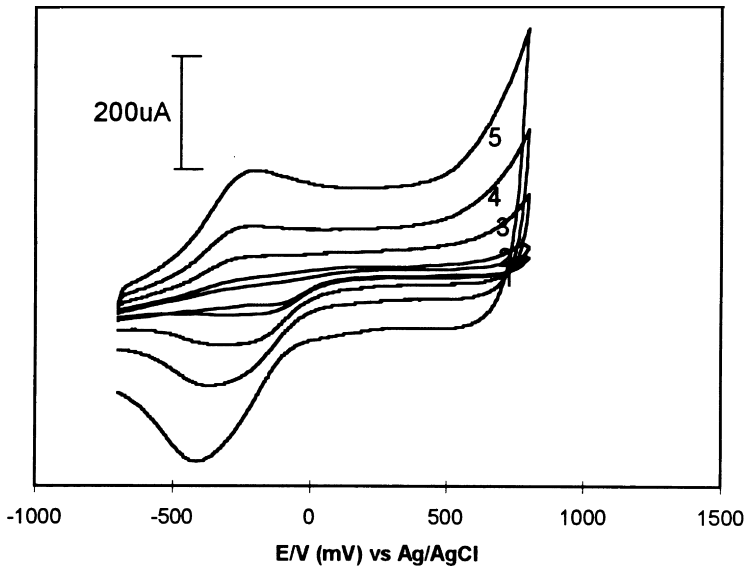

Fig. 6. CVs of 30-min deposited PPY on PSS surface, prior to the deposition of ITO coated glass surface in 0.1 KCl.

electrical conductivity was measured by simply contacting two different points of the sample deposited on glass substrates. In order not to introduce some problems related to the contacts, PPY films were deposited on interdigitated electrodes prepared so that the interdigitated chromium electrode metals did not diffuse in the PPY films. The interdigitated electrodes were of the same size and had equal separation from one strip to another. The electrical measurements of PSS/PPY films on such types of interdigitated electrodes were investigated. The stability in electrical measurement as a function of time of self-assembled PPY is observed as shown in Fig. 8. *I–V* characteristics reveal an

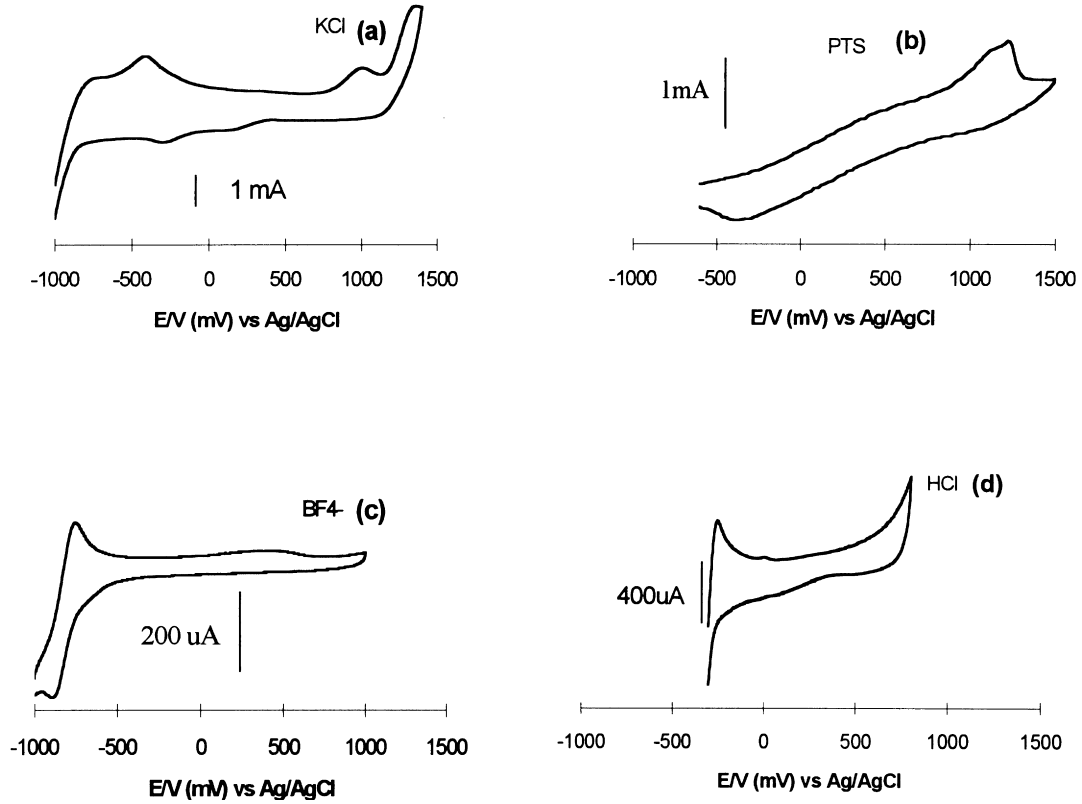

Fig. 7. Cyclic voltammogram of PPY in different electrolytes at a scan of 50 mV/s using Ag/AgCl as a reference electrode and platinum as counter, vs. KCl, PTS, BF_4^- and HCl.

Table 3
Electrochemical parameters of PPY films in different electrolytic media

Electrolytes	Concentration of electrolytes (M)	Applied potential (V)	Oxidation potential (mV)	Reduction potential (mV)
KCl	0.1	−1.0 to 1.4	1067.6, 174.5, −305.8	982.2, −412.5, −771.9
PTS	0.026	−0.6 to 1.5	1396.5, 652.8, 528, −542.8	1008.6, −375.5
BF_4^-	0.1	−1.0 to 1.0	987.3, 332.0, −894.1	932.8, 386.8, −759.9
HCl	0.001	−0.3 to 0.8	−588.0, −331.94	−692.2, 31.94

ohmic behaviour. Interestingly, the *I–V* characteristics are found to be increasing for the film during the next days of the measurements; this could be related to the removal surface water from the films. Further drying of the PPY films in ambient condition showed an increase in the *I–V* characteristics and later, a constant behaviour for a period of 30 days. The self-assembled films are as stable as the electrochemically or the chemically synthesized films. The estimated conductivity of the samples was found to be between 10^{-1} and 10^{-2} S/cm depending upon the thickness of the film.

The change in the electrical behaviour was assumed as a function of dedoping in aqueous ammonia. Fig. 9a shows such dedoping effect of PPY films as a function of time. The ex-situ *I–V* measurements of PPY films on interdigitated electrodes were observed after the treatment in aqueous ammonia. The films were washed and dried before the *I–V* measurement. The *I–V* characteristics revealed a difference in the dedoping time period for self-assembled films when compared to electrochemically deposited PPY films. The self-assembled films needed longer time for the dedoping because it formed compact films due to the electrostatic interaction of PSS and PPY. The HCl redoping of PPY films at different concentrations is shown in Fig. 9b. The redoping of the films were performed for 5 min at different concentration of HCl, and the *I–V* characteristics of such dedoped films were recorded. It observes the effect of redoping for each treatment in various concentration of HCl. The linearity in *I–V* characteristics of PPY films treated at (10^{-6} M) can be exploited for the use of the film in HCl sensor. Such a result highlights that charge transport is not only related to the doping state but also to the microscopic structure of the PPY film. The *I–V* characteristics of PSS/PPY bilayers also showed change in the magnitude of the current for deposited bilayers.

4. Conclusions

In this work the in-situ self-assembly technique has been successfully applied to obtain ultrathin films of PPY. Although it has been impossible to know the real organization of the polymer at the PSS/substrate or in PPY/PSS structures, the investigation carried out made it possible to speculate about the uniformity of self-assembled films of PPY conducting polymer, and to study some main features linked to the uniformity and the structure of the film, and its doping process. The UV–visible absorption and nanogravimetric results obtained for either PPY deposited as a function of time on PSS/substrate and layer-by-layer with PSS on the substrate were found to be highly reproducible. Nearly equal distributions of grain size of PSS/PPY films were confirmed by AFM and STM study. The diffusion coefficients were calculated to be 1.13 and 3.13 cm^2/s.

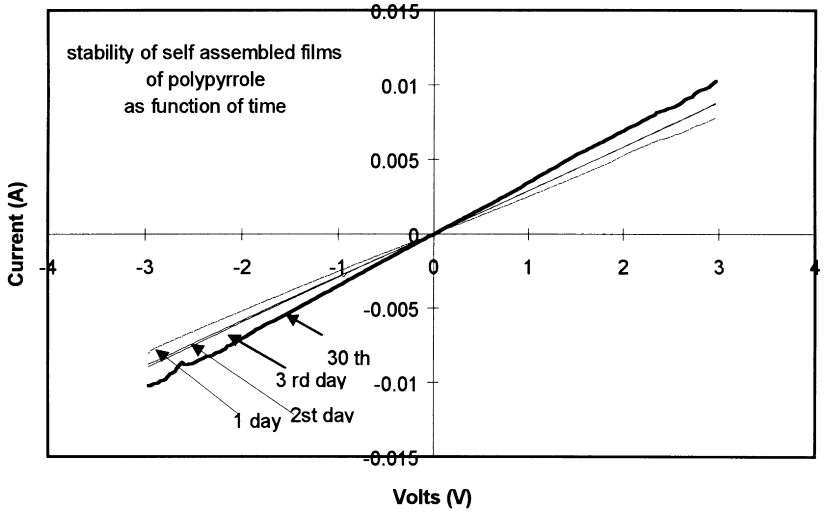

Fig. 8. Current–voltage (*I–V*) characteristics of 30-min self-assembled films on interdigitated electrodes as a function of time.

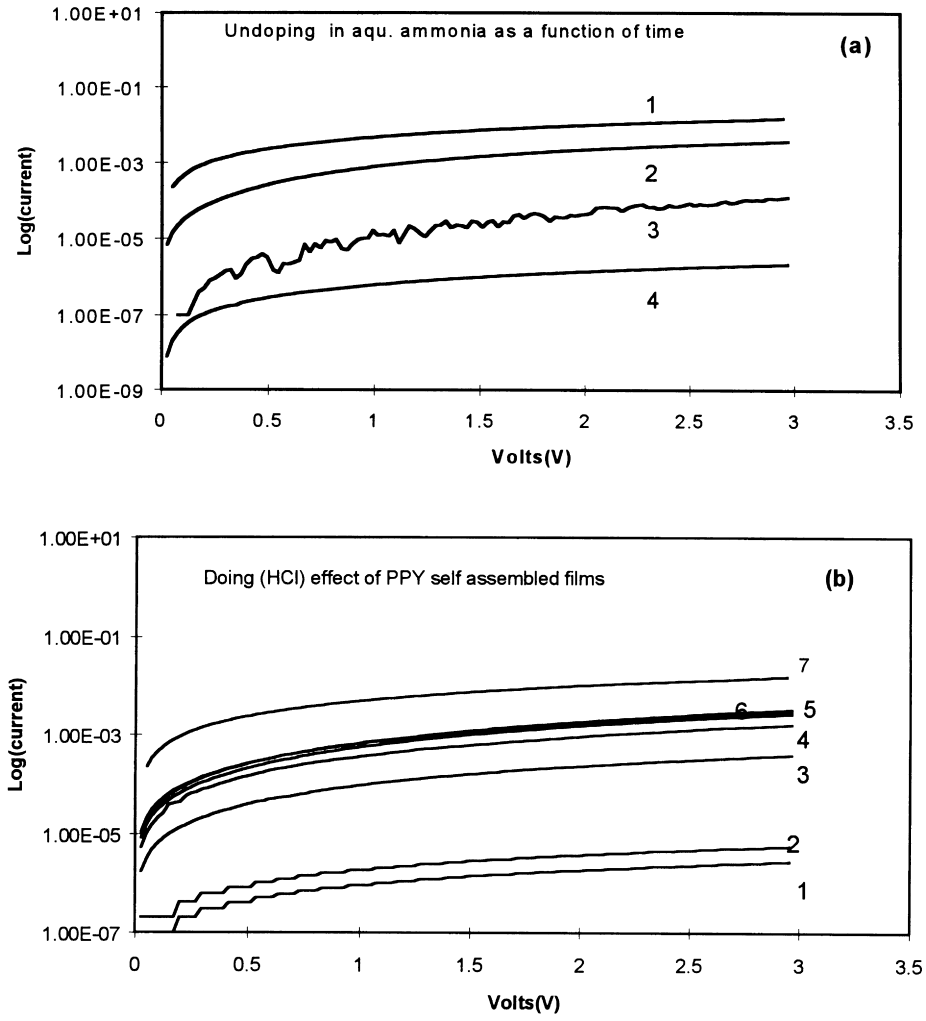

Fig. 9. (a) *I–V* characteristics of dedoping effect of self-assembled films of PPY as a function of time, i.e. 1 (as made), 2 (12 h), 3 (24 h) and 4 (48 h). (b) *I–V* characteristics of self-assembled films of PPY as a function of doping with various concentration of HCl: (1) 10^{-6} M; (2) 10^{-5} M; (3) 10^{-4} M; (4) 10^{-3} M; (5) 10^{-2} M; (6) 10^{-1} M; (7) 1.0 M, respectively.

Typical multilayer films observed the conductivity value in the range of 10^{-1}–10^{-2} S/cm. Such films take longer time in swelling and dedoping processes. The linearity in *I–V* characteristics in the range of 1–10^{-6} M HCl of the treated PPY films could be exploited as a HCl sensor. Furthermore, the possibility of knowing and/or controlling parameters like the stability of the film, the packing degree of the molecules organized in film or the morphological features, allow one to overcome design problems crucial for the preparation of homogeneous and highly ordered layered, structures with a low concentration of defects. In fact, these features make it possible to design molecular assemblies of PPY conducting polymer aimed at practical purposes, such as molecular devices and special coatings.

Acknowledgements

The authors are grateful to Drs Sartore, Sergio and Ding for their criticisms during the writing of the manuscript and sincere help in carrying out the experiments. We are thankful to Mr M. Salerno for the AFM measurements on various PPY samples. Thanks are also due to Mrs M. Panza and D. Nardelli for their technical support. Financial supports from Fondazione Elba (Chapter 2102 of Ministry of Univ. and Research of Italy) and Murst-PST contract on Neural Net Work to Polo Nazionale Bioelettronica are gratefully acknowledged.

References

[1] Ulman A. An introduction to ultrathin films, from Langmuir–Blodgett to self assembly. Boston: Academic Press, 1991 (440pp.).
[2] Roberts GG. Langmuir–Blodgett films. New York: Plenum Press, 1990.
[3] Decher G. Comprehen Supramol Chem 1996;9:507–28.
[4] Decher G. In: Sauvage J-P, Hosseini MW, editors. Templating, self-assembly and self-organization, Oxford: Pergamon Press, 1996.

[5] Decher G. Science 1997;277:1232–7.
[6] Mrksich M. Curr Opin Colloid Interface Sci 1997;2(1):83–8.
[7] Stupp SI. Curr Opin Colloid Interface Sci 1997;3(1):20–6.
[8] Decher G, Eckle M, Johannes Schmitt J, Struth B. Curr Opin Colloid Interface Sci 1998;3:32–9.
[9] Lvov Yu, Decher G. Sukhorukov. Macromolecules 1993;26:5396–9.
[10] Decher G, Hong J, Schmitt J. Thin Solid Films 1992;210/211:831–5.
[11] Chen W, McCarthy TJ. Macromolecules 1997;30(1):78–9.
[12] Decher G, Hong J-D. Makromol Chem Macromol Symp 1991;46:321–7.
[13] Keller SW, Kim H-N, Mallouk TE. J Am Chem Soc 1994;116:8817–8.
[14] Kleinfeld ER, Ferguson GS. Science 1994;265:370–3.
[15] Schmitt J, Decher G, Dressick WJ, Brandow SL, Geer RE, Sashidhar R, Calvert JM. Adv Mater 1997;9:61–5.
[16] Knoll W. Curr Opin Colloid Interface Sci 1996;1:137–43.
[17] Decher G. Science 1997;277:1232–7.
[18] Kellog GJ, Mayes AM, Stockton WB, Ferreira M, Rubner MF, Satija SK. Langmuir 1996;12:5109–13.
[19] Cheung JH, Fou AC, Rubner MF. Thin Solid Films 1994;244:985–9.
[20] Fou AC, Onitsuka O, Ferreira M, Rubner MF, Hsieh BR. J Appl Phys 1996;79:7501.
[21] Ferreira M, Cheung JH, Rubner MF. Thin Solid Films 1994;244:806–9.
[22] Ferreira M, Rubner MF. Macromolecules 1995;28:7107–14.
[23] Fou AC, Rubner MF. Macromolecules 1995;28:7115–20.
[24] Cheung JH, Fou AC, Rubner MF. Thin Solid Films 1994;244:895.
[25] Raposo M, Pontes RS, Mattoso LHC, Oliveira Jr. ON. Macromolecules 1997;30(2):6095–101.
[26] Ram MK, Salerno M, Adami M, Faraci P, Nicolini C. Langmuir 1999;15(4):1252.
[27] Fou AC, Rubner MF. Macromolecules 1995;28:7115–20.
[28] Cheung JH, Stockton WB, Rubner MF. Macromolecules 1997;30(9):2712–6.
[29] Stockton WB, Rubner MF. Macromolecules 1997;30(9):2717–25.
[30] Hong H, Davidov D, Avany Y, Chayet H, Faraggi EZ, Neumann R. Adv Mater 1995;7:846–9.
[31] Fou AC, Onitsuka FM, Howie D, Rubner MF. Polym Mater Sci Engng 1995;72:160.
[32] Skotheim TA, editor. Handbook of conducting polymers New York: Marcel Dekker, 1986.
[33] Kohlman RS, Joo J, Epstein AJ. In: Mark JE, editor. Physical properties of polymers handbook, New York: American Institute of Physics, 1996 (453pp. and references therein).
[34] Burroughes JH, Jones CA, Friend RH. Nature 1988;335:137.
[35] Baughman RH, Shacklette LW, Elsenbaumer RL, Plichta EJ, Becht C. In: Lazarev PI, editor. Molecular electronics, Dordrecht: Kluwer Academic, 1991.
[36] Otero TF, Rodriguez. In: Aldissi M, editor. Intrinsically conducting polymers: an emerging technology, Dordrecht: Kluwer Academic, 1993.
[37] See, for example, the Proceedings of the 1992 International Conference on Synthetic Metals, 1993:55–7.
[38] Ram MK, Annapoorni S, Malhotra BD. J Appl Polym Sci 1996;60:407.
[39] Ramnathan K, Ram MK, Verghese MM, Malhotra BD. J Appl Polym Sci 1996;60:2309–16.
[40] Ram MK, Sundaresan NS, Vardhan HH, Malhotra BD. J Mater Sci Lett 1996;15:997–1000.
[41] Beladakere NN, Misra SCK, Ram MK, Gupta R, Rout DK, Malhotra BD, Chandra S. J Phys: Condens Matter 1992;4:5747.
[42] Ram MK, Adami M, Sartore M, Paddeu S, Nicolini C. Presented in the Foresight Conference 1997.
[43] Ram MK, Adami M, Sartore M, Salerno M, Paddeu S, Nicolini C. Synth Met, 1999;100:249.
[44] Orata D, Buttry DA. J Am Chem Soc 1987;109:3574.
[45] Zhigang Q, Pickup PG. Chem Mater 1997;9:2934–9.
[46] Misra SCK, Beladakere NN, Pandey SS, Ram MK, Sharma TP, Malhotra BD, Chandra S. J Appl Polym Sci 1993;50:411.
[47] Bredas JL, Scott JC, Yakushi K, Street GB. Phys Rev B 1984;30:1023–5.
[48] Yakushi K, Lauchlan LJ, Clarke TC, Street GB. J Chem Phys 1983;79:4774–8.
[49] Ram MK, Sundaresan NS, Malhotra BD. J Mater Sci Lett 1994;13:1490–3.
[50] Verghese MM, Ram MK, Vardhan H, Ashraf A, Malhotra BD. Polymer 1997;38(7):1625–9.
[51] Paddeu S, Ram MK, Carrara S, Nicolini C. Nanotechnology 1998;9:228–36.
[52] Yang C, Dong S. Electroanalysis 1998;10(3):173–6.
[53] Iseki M, Saito K, Kurube K, Mizukami A. Synth Met 1991;40:117.
[54] Maeda S, Armes SP. J Colloid Interface Sci 1993;159:257.
[55] Satoh M, Kaneto K, Yoshinom K. Synth Met 1986;14:289.